

SUPPORTING INFORMATION

Na–Ni–H Phase Formation at High Pressures and High Temperatures: Hydrido Complexes $[\text{NiH}_5]^{3-}$ Versus the Perovskite NaNiH_3

Kristina Spektor,^{1,*} Wilson A. Crichton,¹ Stanislav Filippov,^{2,3} Johan Klarbring,² Sergei I. Simak,² Andreas Fischer,⁴ and Ulrich Häussermann^{3,*}

¹ ESRF, The European Synchrotron Radiation Facility, F-38000 Grenoble, France

²Theoretical Physics Division, Department of Physics, Chemistry and Biology (IFM) Linköping University, SE-581 83, Linköping, Sweden

³Department of Materials and Environmental Chemistry, Stockholm University, SE-10691 Stockholm, Sweden³

⁴Department of Physics, Augsburg University, D-86135 Augsburg, Germany

*E-mails: Kristina.Spektor@gmail.com; Ulrich.Haussermann@mmk.su.se

Figure S1. Splitting of 220 reflection of the cubic HT-HP Na_3NiH_5 during the transition to LT-HP polymorph.

Figure S2. Formation of LP Na_3NiH_5 during decompression of the 5 GPa run to ambient.

Figure S3. Fragment of a 2D-PXRD pattern of LP Na_3NiH_5 product.

Details of structure solution of “ Na_3Ni ” arrangement in LP Na_3NiH_5 .

Figure S4. Deviatoric stress as a function of the simulation time for HT-HP Na_3NiH_5 .

Figure S5. Probability map of angular positions of each H atom in all NiH_5^{3-} complexes of the HT-HP and LT-HP phases.

Details of the Rietveld refinement procedures for Na–Ni–H products.

Figure S6. Results of the Rietveld fit of cubic HT-HP Na_3NiH_5 model to *in situ* PXRD data at 365 °C, ~5 GPa.

Figure S7. Results of the Rietveld fit of *Cmcm* LT-HP Na_3NiH_5 model to *in situ* PXRD data at 320 °C, ~5 GPa (a) and RT, ~4.4 GPa (b).

Figure S8. Phase fractions of Na–Ni–H products and nickel hydride as a function of time and temperature during the 10 GPa experiment.

Figure S9. Experimental and computed EOS for NaNiH_3 .

Figure S10. Magnified high angle region of the NaNiH_3 perovskite structure Rietveld fit.

Figure S11. FWHM values for NaNiH_3 diffraction peaks as a function of 2θ at ambient p , T .

Figure S12. DFT-computed decomposition enthalpies for Na_3NiH_5 and Na_2NiH_4 .

Figure S13. Electronic band structure (a) and phonon dispersions (b) for NaNiH_3 and LiNiH_3 .

Table S1. Fractional coordinates and atomic displacement parameters obtained for the perovskite NaNiH_3 .

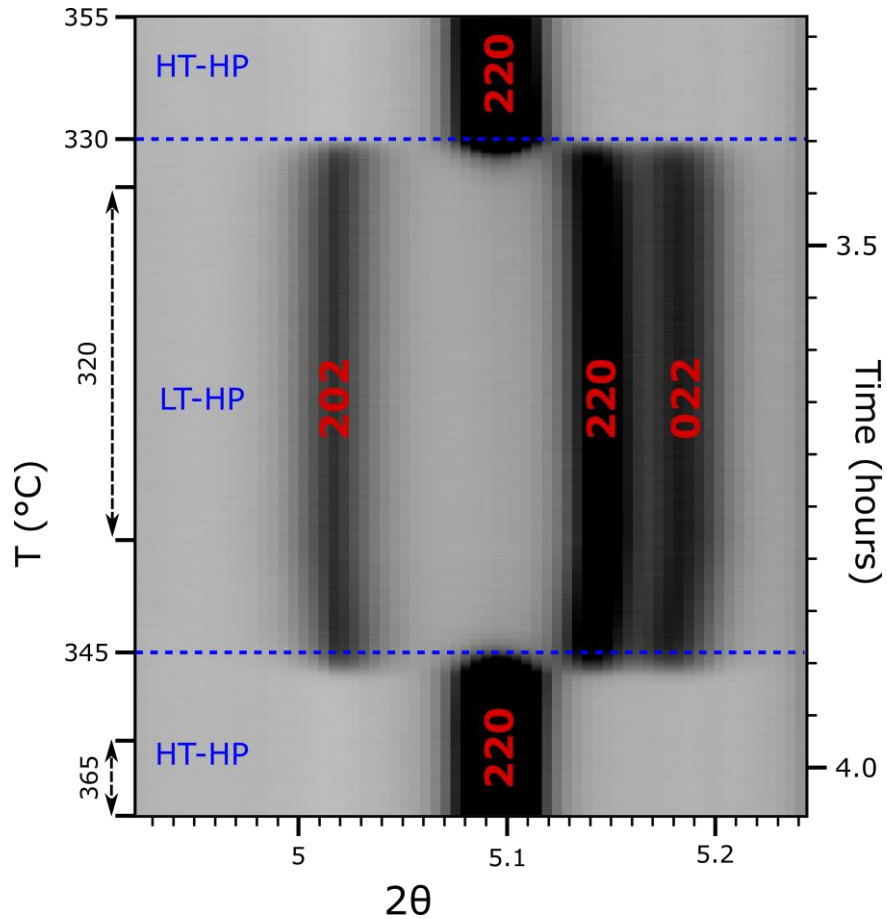


Figure S1. A close up of *in situ* PXRD data collected at ~ 5 GPa ($\lambda = 0.22542$ Å), showing the splitting and reappearance of 220 reflection of the cubic HT-HP Na_3NiH_5 during its forward transformation to the orthorhombic LT-HP polymorph on cooling and the reverse transformation on reheating, respectively.

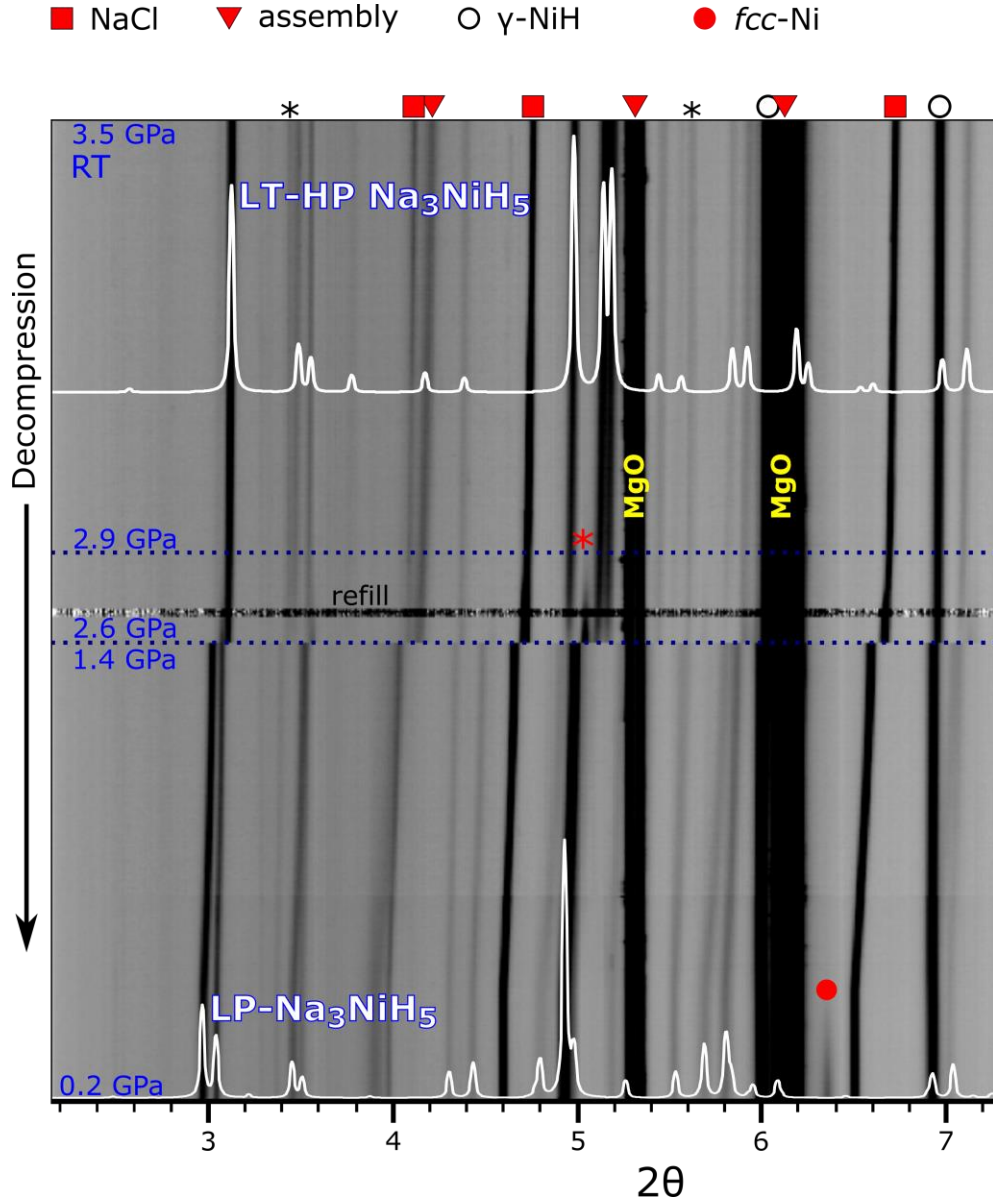
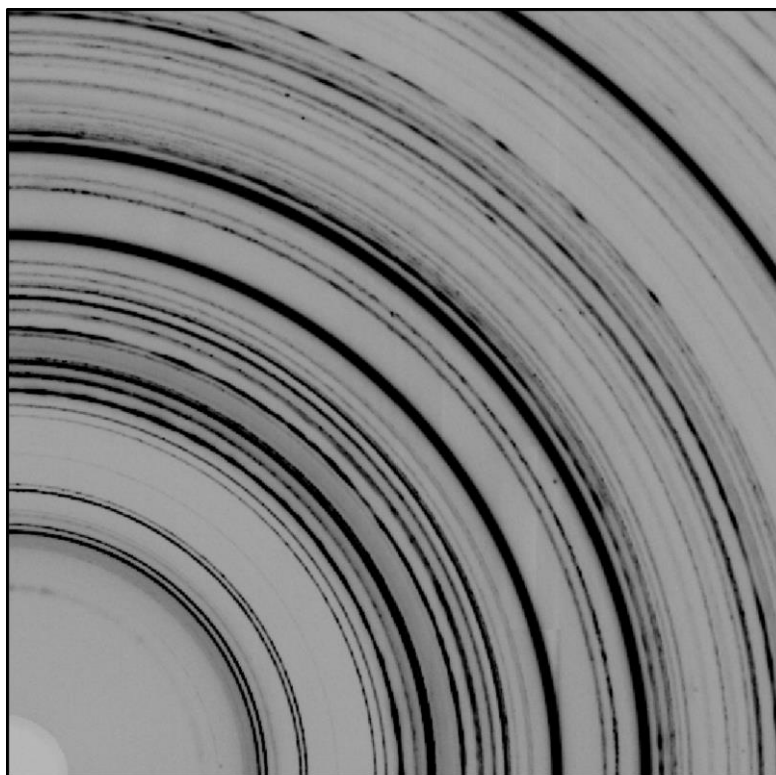


Figure S2. Compilation of *in situ* PXRD patterns ($\lambda = 0.22542 \text{ \AA}$) showing the transformation of LT-HP Na_3NiH_5 to the LP polymorph on decompression following the 5 GPa experiment. Only a part of the decompression data, starting from ~ 3.5 GPa, is shown. Simulated PXRD patterns of LT-HP and LP Na_3NiH_5 phases (white) are displayed over the data. A rapid pressure drop from 2.6 to 1.4 GPa occurred during the decompression, which is likely due to leftover hydrogen escaping the capsule. Red asterisk marks the appearance of the strongest LP Na_3NiH_5 peak, indicating onset of the transformation. Peaks of unknown minor impurities are noted with black asterisks.



2θ (°) —————→

Figure S3. Fragment of 2D PXRD pattern collected at ID15B, ESRF ($\lambda = 0.41127$ Å) showing the 5 GPa run product recovered at ambient p , T . The product contains the LP Na_3NiH_5 phase as a major ternary compound along with leftover Ni and NaH. The texture contribution to LP Na_3NiH_5 diffraction and peak overlap with other phases do not appear significant. The integrated 1D pattern was used for indexing and subsequent structure solution of LP Na_3NiH_5 .

Details of structure solution of “Na₃Ni” arrangement in LP Na₃NiH₅.

The primary attempt to solve the Na–Ni metal arrangement in LP Na₃NiH₅ was made using Superflip algorithm¹ in Jana2006² software. The procedure was performed within the space group *Pnma*, previously established via Le Bail analysis³ and subsequent space group tests in Jana2006. A well-reproducible solution yielded an arrangement of 3Na:1Ni stoichiometry where the Ni atom occupied the 4*c* Wyckoff site, and Na atoms were located at 4*c* and 8*d* Wyckoff sites ($Z = 4$). The obtained structure was used for the Rietveld refinement⁴ against the experimental data (refinement details are provided in the corresponding section of SI). The structure solution obtained via Superflip overall fitted reasonably close to the observed diffraction pattern; however, several weak peaks have shown noticeable intensity mismatch, while the best R_{obs} was at $\sim 11.5\%$. Interestingly, the cell parameters of LP Na₃NiH₅ were found to match closely those of potassium orthonitrate, K₃NO₄, which also crystallizes in *Pnma* space group ($a = 10.921 \text{ \AA}$; $b = 7.952 \text{ \AA}$; $c = 5.667 \text{ \AA}$).⁵ The Wyckoff sites of the 3 K (4*c*, 8*d*) and 1 N atom (4*c*) are coincident with those of the “Na₃Ni” arrangement derived via Superflip. The two atomic arrangements are very similar and contain the same “A₃B” building units, yet the stacking of these units is essentially different. Once the fractional coordinates of potassium and nitrogen atoms from K₃NO₄ structure were adopted for Na and Ni positions, respectively, the Rietveld fit has improved significantly, yielding the $R_{\text{obs}} \sim 7.7\%$, while the intensity mismatch became negligible. The resulting “Na₃Ni” structure was further used as a base for exploring possible hydrogen arrangements via simulated annealing (SA) global optimization algorithm in Endeavour 1.7 software.⁶

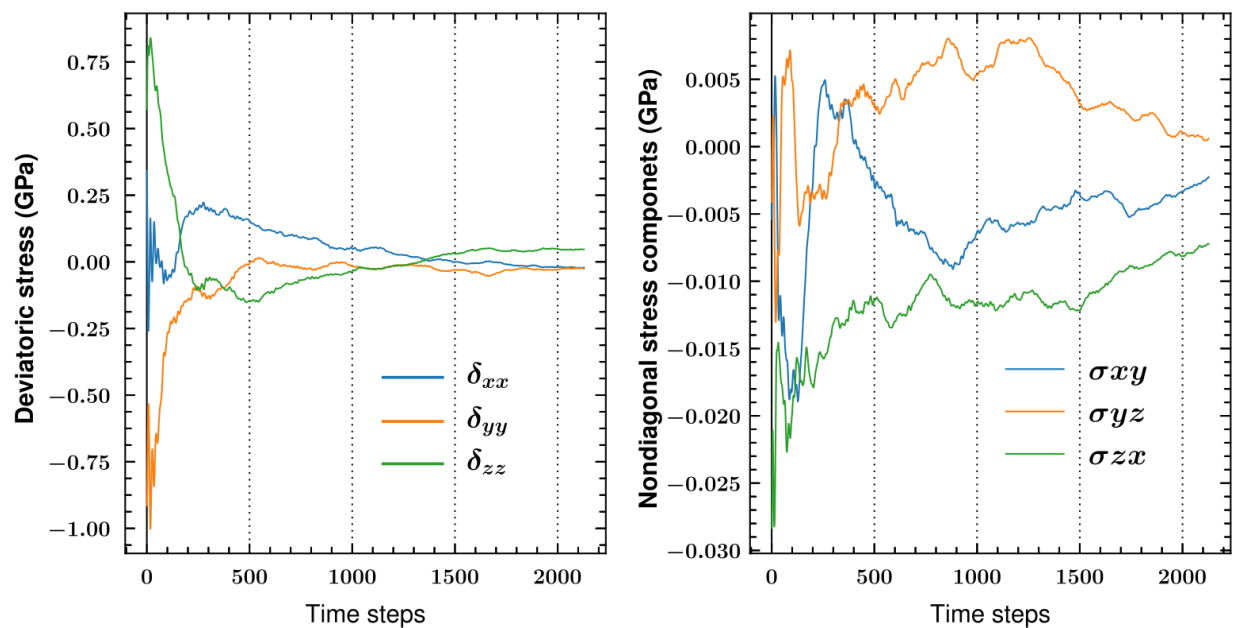


Figure S4. Running averages of deviatoric stress, diagonal (left), and non-diagonal components (right) of the stress tensor as a function of the simulation time (1 time step = 1 fs) for HT-HP Na_3NiH_5 .

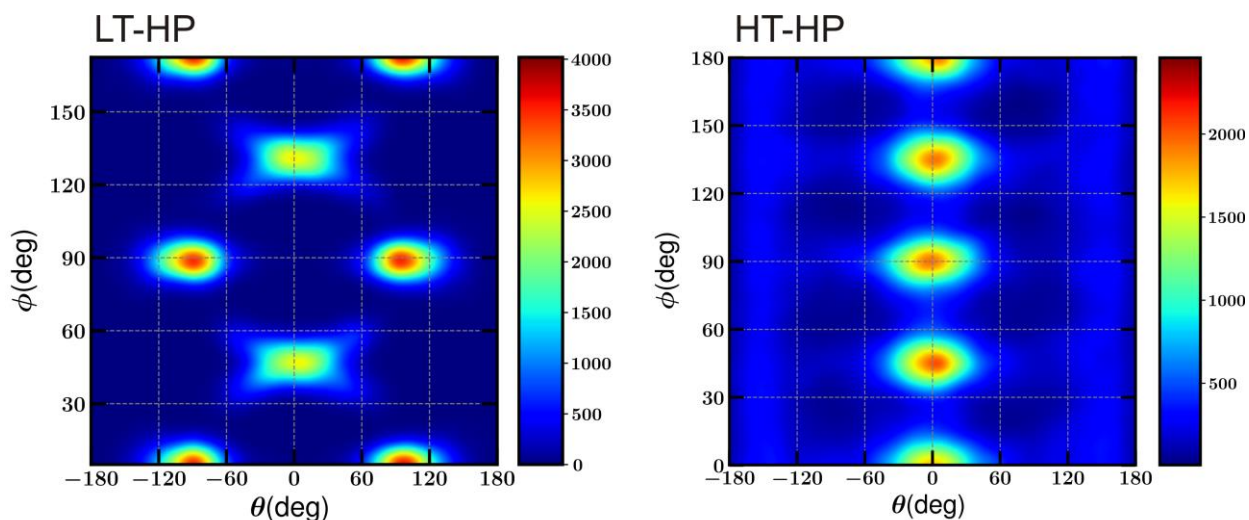


Figure S5. 2D histogram of angular positions of H atoms in the NiH_5^{3-} complexes. Theta is azimuth, i.e. it is defined as angle between the z-axis of the simulation cell and the direction from Ni to the H atom at \mathbf{R}_i . Phi is the polar angle, i.e. the angle between the projection of \mathbf{R}_i on the xy-plane and the x-axis of the simulation cell. The angular pair (phi, theta) for each H in each NiH_5^{3-} complex was identified and added to the final dataset, which resulted in the 2D histograms shown above. Brighter colors mean the presence of H atoms at certain combinations of (theta, phi), whereas dark blue means that these values were never observed. In HT-HP Na_3NiH_5 (right panel) the H atoms of the complexes perform rotations, both with azimuthal and polar angles. However, as evident from the color code, the H atoms do not spend much time in those positions, which are collectively swapped. This manifests reorientational dynamics of the complexes. Contrary, in LT-HP Na_3NiH_5 (left panel) the H atoms of the complexes keep their average positions and oscillate around them.

Details of the Rietveld refinement procedures for Na–Ni–H products

Rietveld refinement⁴ for all Na–Ni–H products was performed using Jana2006 package.² For the refinements of LT-HP and HT-HP Na₃NiH₅ structures (patterns collected *in situ* at ID06-LVP, ESRF, $\lambda = 0.22542 \text{ \AA}$) a manually created background was used, while refined parameters included unit cell dimensions, Gaussian and Lorentzian components of the pseudo-Voigt peak shape profile, atomic displacement parameters (U_{iso}). In case of LT-HP Na₃NiH₅ refinement, fractional coordinates of Na and Ni atoms were refined as well. The ADPs of Na atoms were constrained together for both cubic and orthorhombic polymorph. The positions of H atoms remained fixed during the refinement as well as their ADPs, which were set to $U_{\text{iso}}=0.038 \text{ \AA}^2$ ($B_{\text{iso}} \approx 3 \text{ \AA}^2$). For both LT-HP and HT-HP phases, the regions of the patterns containing assembly peaks were excluded from the refinement. In addition to Na₃NiH₅ compounds, nickel hydride and sodium chloride structures were included in the refinement, albeit most of NaCl reflections were excluded as well. The results of refinements are shown in Figures S6 (HT-HP Na₃NiH₅ at 365 °C, ~5 GPa) and S7a,b (LT-HP Na₃NiH₅ at 320 °C, ~5 GPa and RT, ~4.4 GPa). During the initial Rietveld analysis of hypothetical “Na₂Ni₂” and “Na₃Ni” metal arrangements, which yielded respective non-stoichiometric “Na₂Ni_{~1.3}” and “Na_{2.7}Ni” compositions, the same procedure was used. In addition, the occupancy of either Na or Ni atom at *4b* or *4c* site in *Fm-3m* or *Cmcm* structure, respectively, was refined. The ADPs were constrained together for the atoms of the same type.

During the Rietveld analysis of “Na₃Ni” metal arrangements in LP Na₃NiH₅ structure (PXRD collected at ID15B, ESRF, $\lambda = 0.41127 \text{ \AA}$) the following parameters were refined: 6th degree polynomial background; unit cell parameters; Gaussian and Lorentzian components of the pseudo-Voigt peak shape profile; fractional coordinates for Na and Ni atoms and their isotropic ADPs (U_{iso}). During the refinement the U_{iso} of Na atoms were constrained together. The regions of the pattern containing minor impurity peaks were excluded. The *fcc*-Ni metal and sodium hydride (NaH) structures were added to the refinement as well. Rietveld refinement of the DFT-optimized LP Na₃NiH₅ followed the same protocol, while the coordinates of H atoms remained fixed during the procedure and their U_{iso} were constrained to 0.038 \AA^2 ($B_{\text{iso}} \approx 3 \text{ \AA}^2$).

The Rietveld refinement of NaNiH₃ perovskite structure (against high resolution PXRD collected at ID22, ESRF, $\lambda = 0.3544 \text{ \AA}$) included: 8-degree polynomial background; zero shift; NaNiH₃ unit cell parameter; components of Lorentzian peak shape function; ADPs (U_{iso}) of Na and Ni atoms. As in the other refinements of Na–Ni–H structures, U_{iso} parameters for H atoms were fixed at 0.038 \AA^2 ($B_{\text{iso}} \approx 3 \text{ \AA}^2$). Broad, low intensity peaks of unreacted nickel as well as minor impurity peaks likely present due to sodium hydroxide surface contamination were excluded from the refinement.

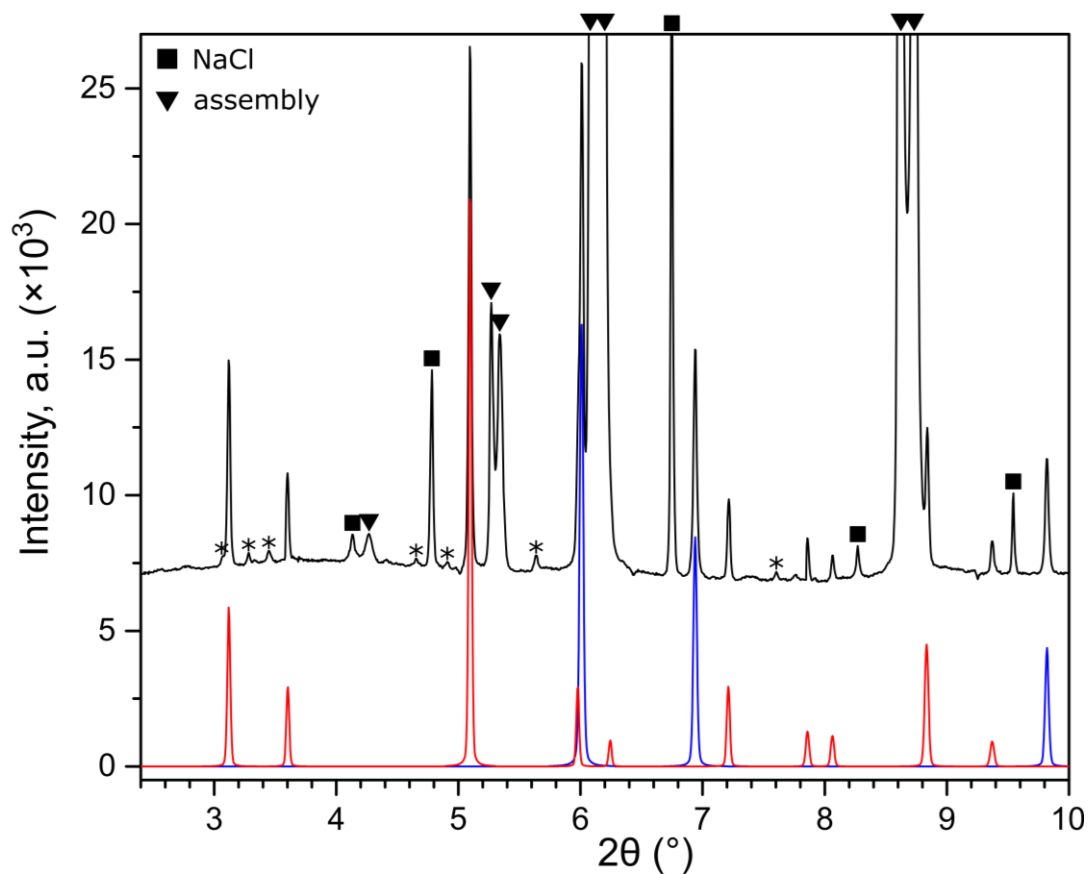


Figure S6. PXRD patterns of HT-HP Na_3NiH_5 (red) and nickel hydride (blue) simulated from the results of Rietveld fit of the corresponding phases to the PXRD data (black) collected *in situ* at ID06-LVP, ESRF, during the temperature dwell at 365 °C, ~5 GPa ($\lambda = 0.22542 \text{ \AA}$). Diffraction peaks corresponding to assembly (MgO, *h*-BN), most of NaCl reflections as well as several low intensity peaks of an unidentified impurity (marked with asterisks) were excluded from the refinement.

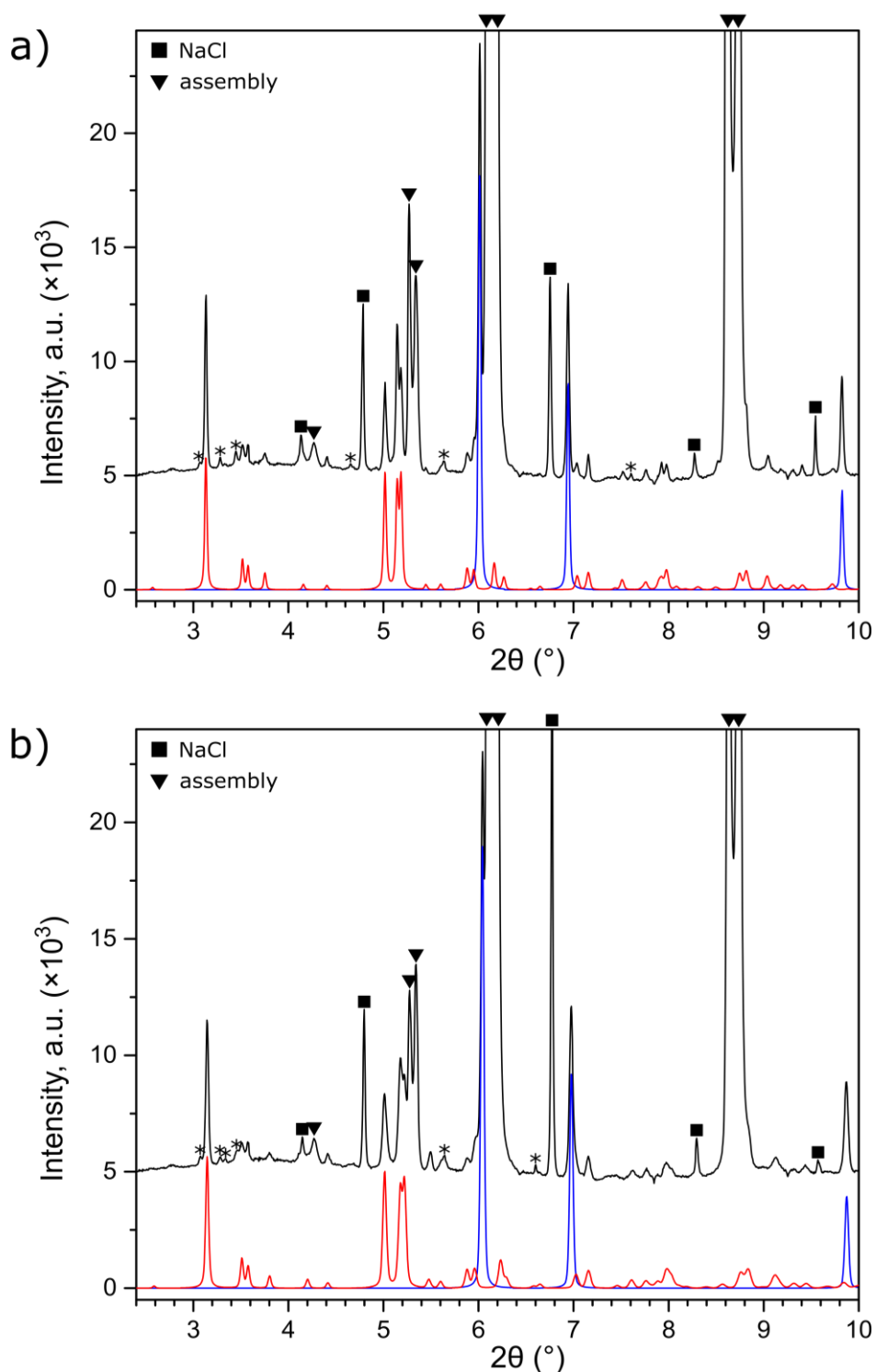


Figure S7. PXRD patterns of LT-HP Na₃NiH₅ (red) and nickel hydride (blue) simulated from the results of Rietveld fit of the corresponding phases to the PXRD data (black) collected *in situ* at ID06-LVP, ESRF ($\lambda = 0.22542 \text{ \AA}$): (a) during the temperature dwell at 320 °C, ~5 GPa and (b) after the temperature quench (RT, ~4.4 GPa). Diffraction peaks corresponding to assembly (MgO, *h*-BN), most of NaCl reflections as well as several low intensity peaks of an unidentified impurity (marked with asterisks) were excluded from the refinement.

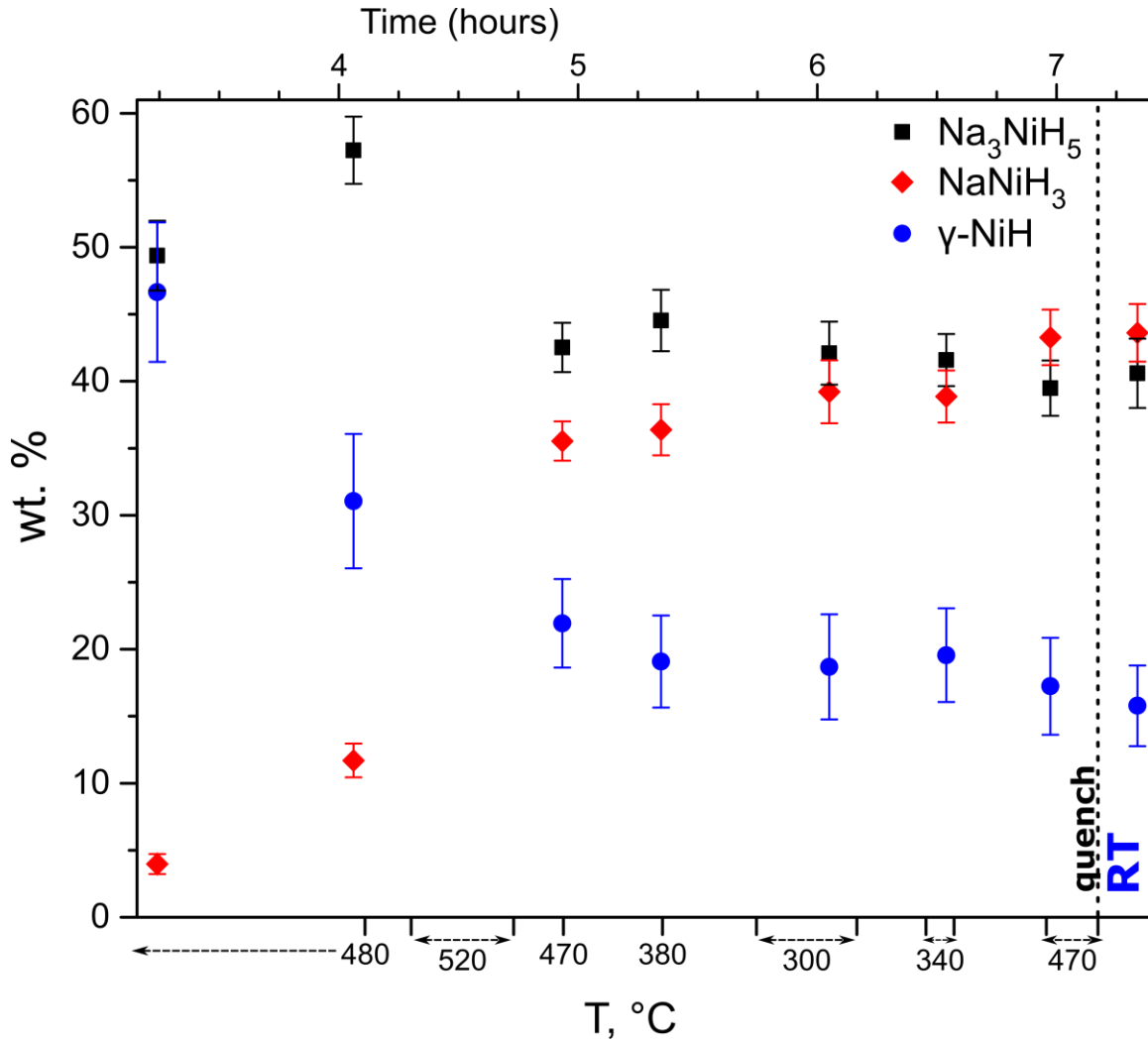


Figure S8. Change in relative phase fractions (weight %) of NaNiH_3 perovskite, Na_3NiH_5 phases (HT-HP or LT-HP, depending on the temperature) and nickel hydride as a function of time and temperature during the 10 GPa run (see Figure 9a in the main text). The phase fractions were extracted via Rietveld refinement using *in situ* PXRD data chosen from the part of the experiment where the three phases coexisted. The PXRD datasets were prepared by averaging 10–11 diffraction patterns collected during temperature dwells. The input structures for the refinement of Na–Ni–H compounds in a mixture were the same as when the phases were refined separately. Regions of overlap with NaCl peaks were excluded from the refinement. The displayed errors correspond to tripled standard deviation ($3\times\sigma$) output from the refinement. The results show that the NaNiH_3 concentration steadily grows through the experiment, while the fractions of the other two compounds keep on decreasing.

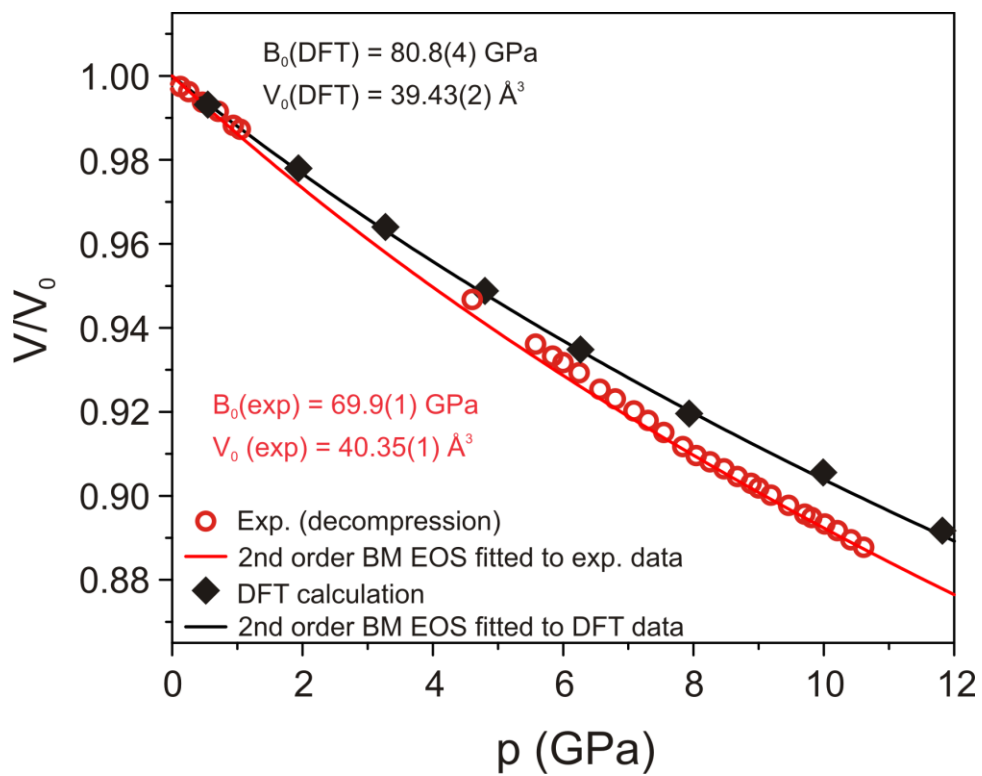


Figure S9. Equation of state for the perovskite NaNiH₃. Experimental and computed values are presented as red circles and black diamonds, respectively.

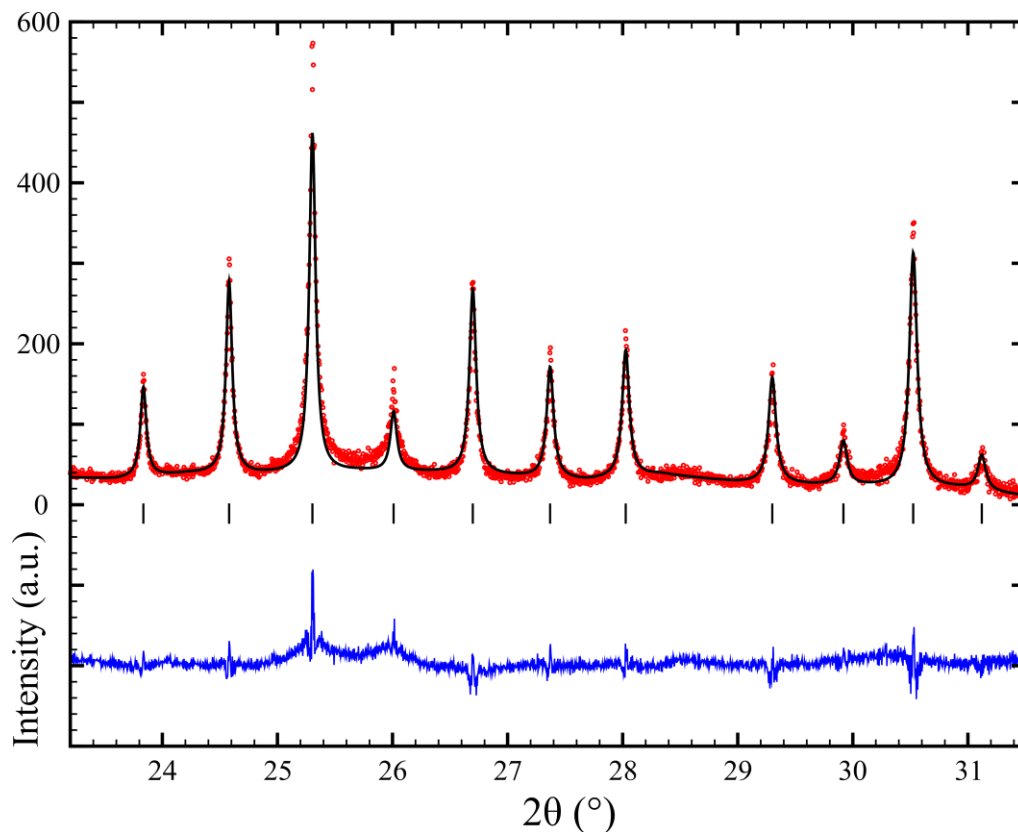


Figure S10. Magnified high angle region of the NaNiH₃ cubic perovskite structure Rietveld fit to the ambient synchrotron PXRD of the product after depressurization of the 12 GPa run ($\lambda = 0.3544 \text{ \AA}$).

Table S1. Fractional coordinates and atomic displacement parameters obtained for the perovskite NaNiH₃. ADPs of hydrogen atoms were set to 0.038 \AA^2 (U_{iso}) and fixed during the refinement.

Atom	Wyck	x	y	z	$U_{\text{iso}} (\text{\AA}^2)$	$B_{\text{iso}} (\text{\AA}^2)$
Ni	$1a$	0	0	0	0.00451(11)	0.36(9)
Na	$1b$	0.5	0.5	0.5	0.0103(3)	0.81(2)
H	$3d$	0.5	0	0	0.038	3

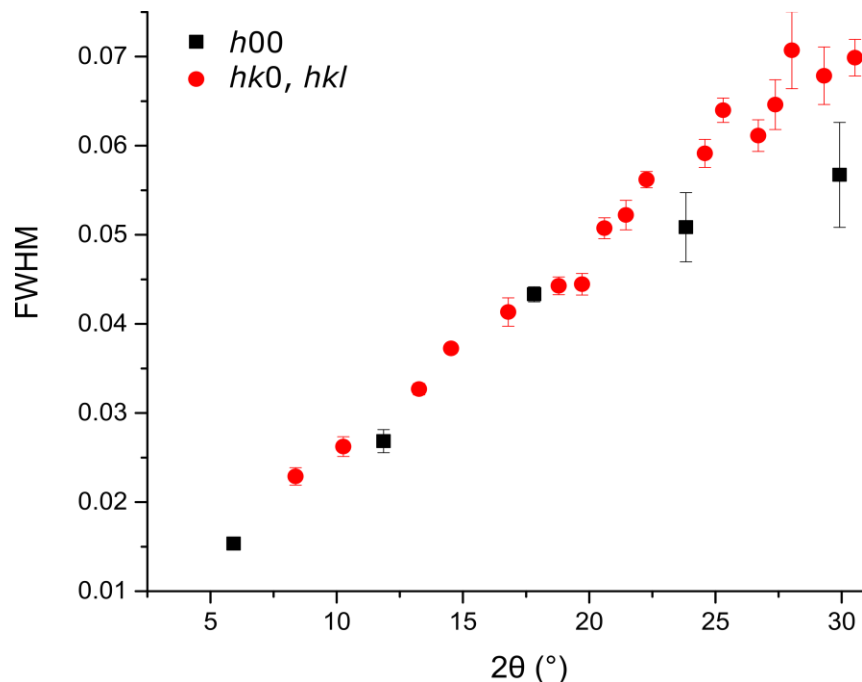


Figure S11. FWHM values of NaNiH_3 perovskite diffraction peaks shown as a function of 2θ angle. The FWHM values extracted from the high resolution PXRD pattern collected at ambient p , T at ID22, ESRF ($\lambda = 0.3544 \text{ \AA}$) by fitting the observed peaks with the Pearson VII function⁷ in the DatLab software.⁸ The errors correspond to $3\times\sigma$ output from the fitting. The $h00$ reflections (black squares) appeared slightly narrower compared to $hk0$ and hkl (red circles), but only by a very small amount. To test for a possible rhombohedral distortion in the cubic NaNiH_3 perovskite, Le Bail analysis³ of ID22 PXRD data using rhombohedral crystal system (SG 160) was performed, yielding the γ angle = $89.990(5)^\circ$. This suggests that any possible distortion is negligible, and perovskite NaNiH_3 can be considered metrically cubic. In addition, the PXRD pattern was tested for superlattice reflections, and none were detected.

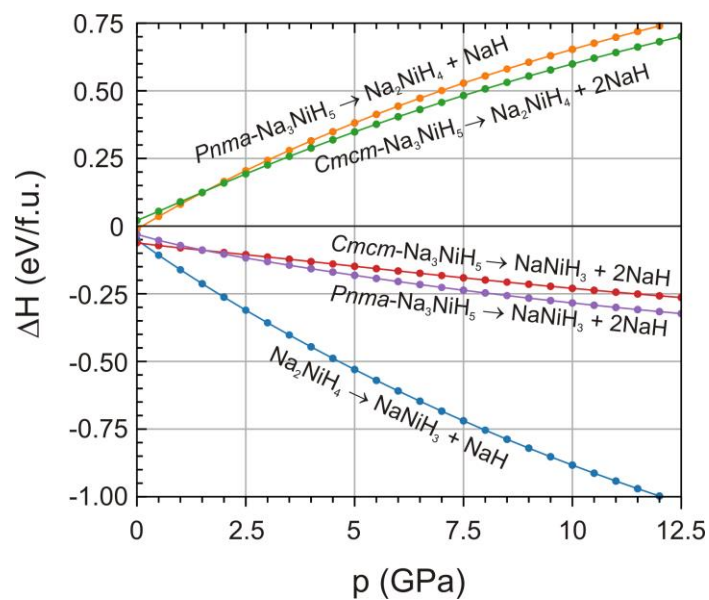


Figure S12. Decomposition enthalpies of Na_3NiH_5 and hypothetical Na_2NiH_4 as a function of pressure. Na_2NiH_4 is not expected as an intermediate in the decomposition of Na_3NiH_5 into NaNiH_3 and NaH .

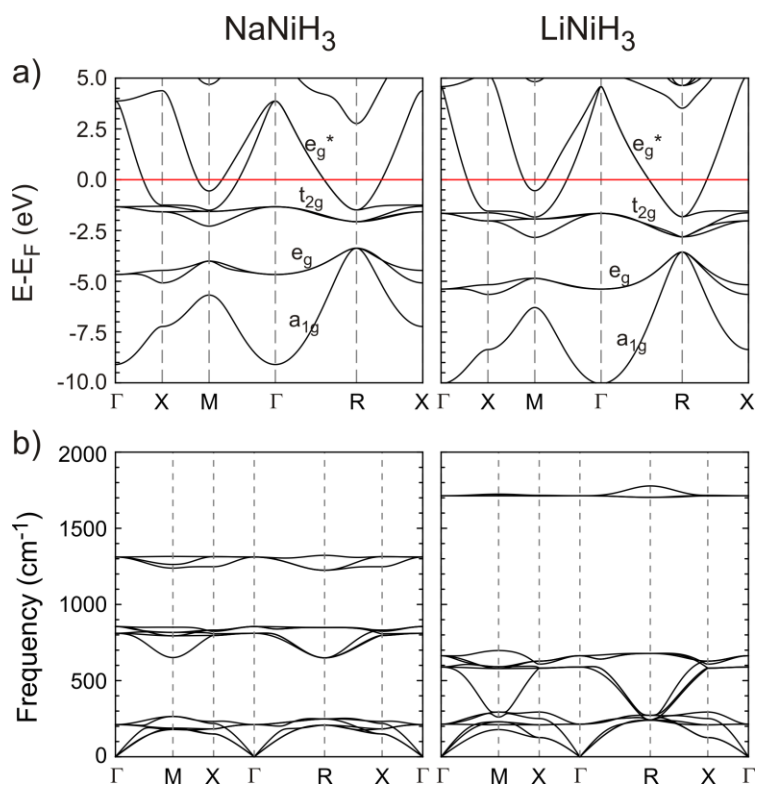


Figure S13. Electronic band structure (a) and phonon dispersions (b) for NaNiH₃ and LiNiH₃ at their respective equilibrium volumes (zero pressure).

References

- (1) Palatinus, L.; Chapuis, G. SUPERFLIP – a Computer Program for the Solution of Crystal Structures by Charge Flipping in Arbitrary Dimensions. *Journal of Applied Crystallography* **2007**, *40* (4), 786–790. <https://doi.org/10.1107/S0021889807029238>.
- (2) Petříček, V.; Dušek, M.; Palatinus, L. Crystallographic Computing System JANA2006: General Features. *Zeitschrift für Kristallographie - Crystalline Materials* **2014**, *229* (5), 345–352. <https://doi.org/10.1515/zkri-2014-1737>.
- (3) Le Bail, A.; Duroy, H.; Fourquet, J. L. Ab-Initio Structure Determination of LiSbWO₆ by X-Ray Powder Diffraction. *Materials Research Bulletin* **1988**, *23* (3), 447–452. [https://doi.org/10.1016/0025-5408\(88\)90019-0](https://doi.org/10.1016/0025-5408(88)90019-0).
- (4) Rietveld, H. M. A Profile Refinement Method for Nuclear and Magnetic Structures. *Journal of Applied Crystallography* **1969**, *2* (2), 65–71. <https://doi.org/10.1107/S0021889869006558>.
- (5) Bremm, Th.; Jansen, M. Einkristallzüchtung und Strukturanalyse von Trikaliumorthonitrat. *Zeitschrift für anorganische und allgemeine Chemie* **1992**, *608* (2), 56–59. <https://doi.org/10.1002/zaac.19926080209>.
- (6) Endeavour – Structure Solution from Powder Diffraction. Crystal Impact – Dr. H. Putz & Dr. K. Brandenburg GbR, Kreuzherrenstr. 102, 53227 Bonn, Germany. <http://www.crystalimpact.com/endeavour>.
- (7) Hall, M. M.; Veeraraghavan, V. G.; Rubin, H.; Winchell, P. G. The Approximation of Symmetric X-Ray Peaks by Pearson Type VII Distributions. *Journal of Applied Crystallography* **1977**, *10* (1), 66–68. <https://doi.org/10.1107/S0021889877012849>.
- (8) Syassen, K. *Computer Code DATLAB*; Max Planck Institute, Stuttgart, Germany, 2003.